Information-Theoretic Model and Analysis of Molecular Signaling in Targeted Drug Delivery

Uche A.K. Chude-Okonkwo, *Member, IEEE*, B.T. Maharaj, *Senior Member, IEEE,* Athanasios.V. Vasilakos, *Senior Member, IEEE*, and Reza Malekian, *Senior Member, IEEE*

***Abstract*— Targeted drug delivery (TDD) modality promises a smart localization of appropriate dose of therapeutic drugs to the targeted part of the body at reduced system toxicity. To achieve the desired goals of TDD, accurate analysis of the system is important. Recent advances in molecular communication (MC) present prospects to analyzing the TDD process using engineering concepts and tools. Specifically, the MC platform supports the abstraction of TDD process as a communication engineering problem in which the injection and transportation of drug particles in the human body and the delivery to a specific tissue or organ can be analyzed using communication engineering tools. In this paper we stand on the MC platform to present the information-theoretic model and analysis of the TDD systems. We present a modular structure of the TDD system and the probabilistic models of the MC-abstracted modules in an intuitive manner. Simulated results of information-theoretic measures such as the mutual information are employed to analyze the performance of the TDD system. Results indicate that uncertainties in drug injection/release systems, nanoparticles propagation channel and nanoreceiver systems influence the mutual information of the system, which is relative to the system's bioequivalence measure.**

***Index Terms*—Molecular communication, Information theory, mutual information, bioequivalence.**

I. Introduction

TARGETED drug delivery (TDD) is a nanomedical concept that is geared towards ensuring that therapeutic drugs are localized to targeted (pathological) parts of the body in a controlled manner using tools and techniques from micro/nanotechnology and nanoscience [1], [2]. The benefits of TDD are that it provides delivery methods that minimize drug toxicity, improve pharmaceutical profile of a drug, facilitate drug localization at a specific site of action, achieve maximum biocompatibility, and reduce loss, [3]. The TDD systems include devices such as nanocarriers, nanoreceivers, micro/nano implants and drug injection machines [4].

To ensure that a TDD system provides the desired performance, the following factors must be taken into consideration. Firstly, the media through which the nanoparticles (nanosystems or molecules) are conveyed to the targeted site need to be understood. Secondly, the primary microenvironment of the targeted cells must be well understood. Thirdly, armed with the knowledge of the media and the microenvironment, the design of the TDD nanosystems (nanocarrier, nanoreceivers, etc.) is carried out. The design is carried out in a way that ensures that (i) the nanoparticles to be transported through the media and operate in the targeted microenvironment are resilience to adverse cardiovascular effects; (ii) the nanocarriers localize at the targeted site; (iii) optimal nanocarrier capacity is achieved; and; (iv) optimal drug release profile is realized.

Recently, the concept of molecular communication (MC) applied to TDD has projected the capability of artificially controlling and monitoring the TDD activities using nanodevices in what is termed *advanced TDD* [5]. Some examples of MC diffusion channel models for the advanced TDD applications as presented in [6], [7]. In [8] an advanced TDD solution model is presented for targeting multiple cancer sites. In the above applications, the accuracy of the signalling among the natural and artificial nanosystems in the TDD system is very crucial to the system's design. This brings us to the issue of information transfer fidelity among the components of the TDD system.

A. Motivation

The fundamental goal of signalling in TDD, like in any communication system is to ensure accurate transmission, reception and processing of information from/by specific nanosystems in the TDD structure. The concept of MC [9], [10] provides a technical platform to evaluate the accuracy of the signalling. In this sense, we can designate a TDD subsystem as the signalling source and another, the receiver. Then we can evaluate the signalling between the two subsystems using communication engineering metrics. The exchange of information can be evaluated at different subsystems' levels along the TDD signalling pathways. For instance, the signalling can be between the injection machine (for nanocarrier administration) and the targeted extracellular space; between the nanocarrier and the receptors on the targeted cell's surface; between the receptors and the nucleus of the cell; across various signalling pathways in the cell; and even between molecules in the cellular signalling pathways.

Typically, modelling and evaluating the fidelity of information exchange among the components subsystems of the TDD is as complex as the information signalling process

Manuscript received May 30, 2019, revised September 4, 2019.

and the operating environment, where so many systems/processes typically interact and interfere with the signalling processes. The diversity of the interfering and interacting systems and phenomena create the need for multivariate analysis of the TDD system. In addition, the TDD system, just like many biological systems is nonlinear. Hence, the complexity, nonlinearity and multivariate characteristics of the TDD system usually makes it difficult to obtain sufficient data to enable precise evaluation and predictable on the system's signaling. Hence, an amenable option for addressing this challenge is to consider probabilistic approach, which provides methods for defining and quantifying information exchange among systems without necessarily requiring detailed knowledge of the system. By relating TDD to communication engineering in general, and MC in particular, engineering tools and probability concepts that are employed for the analysis of complex, nonlinear and multivariate engineering systems can be extended to TDD systems.

Shannon information theory, originally formulated in engineering context has been considered in recent times as a theoretical framework for the analysis and quantification of information exchange among biological entities. For instance, in [11], the rate distortion theory is employed to evaluate biological signalling pathways in cells. Some fundamental concepts and approach in applying information theory to the analysis of biochemical signalling systems are presented in [12], [13]. In [14], information theory is employed to characterize gradient sensing response of cells. In [15], a tutorial on the application of information theoretic concepts to neural signalling is presented. Within the context of MC, a closed-form expression of capacity is derived for the MC system in [16], and for the intercellular signal transduction in [17]. The beauty of Shannon's work is that it applies to any system that can be abstracted to a sender-receiver topology [18], which is applicable to the ideas in this paper.

B. Paper Contributions

In this work, we employ the information theoretic approach to model the information transfer between subsystems in a TDD system, contemporary and advanced. Specifically, we intuitively present information transfer and molecular signalling between some subsystems from the TDD perspective. Based on some defined input probabilities, we employ numerical and stochastic methods to realize the different TDD channels probability models considered in this work. We model the ligand-receptor binding that defines molecular signal reception in nanosystems as a Poisson-binomial distribution, and use same to compute the conditional probability of the receiver system. We also highlight on the *spatial filtering* property of the ligand-reception system for molecular signal processing. We also propose the evaluation of bioequivalence of a TDD process as a function of mutual information.

The rest of this paper is organized as follows. Section II provides some background on TDD and the formulation of the problem addressed in this paper. The probabilistic system model is presented in Section III. In Section IV, the practical realization of the molecular channel models is presented. The concepts of entropies and mutual information measures are discussed in Section V and VI, respectively. Finally, simulation results and discussion are presented in Section VII.

II. Background and Problem Formulation

A. Concise Model of Targeted Drug Delivery System

The controlled delivery of drug to targeted biological systems in the body using nanocarriers can be done using any of the conventional drug delivery modalities. Popular among these modalities include oral ingestion, intravascular injection and pulmonary method depicted in Fig. 1. As stated in [19], the choice of the nanocarrier administration modality is influenced by factors such as the proximity to the targeted site (to ensure minimal inversion), toxicity level (to ensure minimal toxicity), and bioavailability (to ensure delivery of optimum concentration of nanosystems, at minimal toxicity). For an in-depth discussion on the different modalities for delivering nanocarriers to sites in the body, and there pros and cons, the reader is referred to [5], [19].

The scenarios of focus in this paper are shown in Fig.2. We can assume that there are one or more extracellular sites with disease cells that we intend to target for therapeutic purpose. In this work we consider three sites, which we have labeled *A*, *B*, and *C*. The injection machine, injects a number of nanocarriers into the cardiovascular systems, through which the nanocarriers traverse to reach each of the sites. From the perspective of communication engineering, we can consider the injection machine as a transmitter, the blood circulatory system as a communication channel, and the targeted extracellular space as receivers. In this scenario, the injected

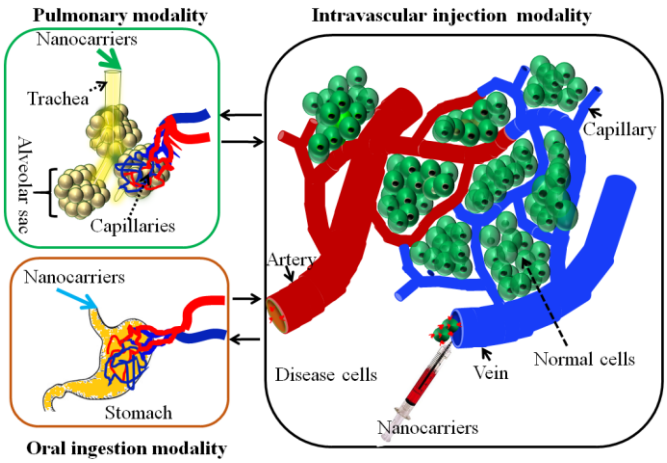

Fig. 1. TDD nanoparticles delivery modalities.

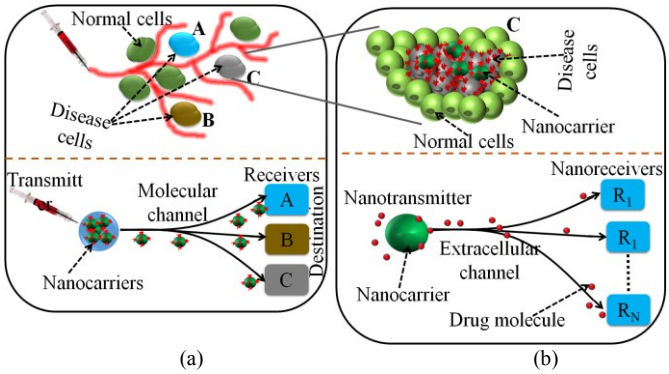

Fig. 2. Communication engineering abstraction of TDD (a) nanocarriers delivery to targeted sites, and (b) nanocarrier targeting of disease cells.

nanocarriers are the information molecules that carry the molecular message meant for delivery to the destinations *A*, *B* and *C* as is depicted in Fig. 2(a). On getting to the targeted site, the nanocarriers, which are equipped with special ligands tethered to their surfaces, bind to complementary receptors that are uniquely expressed by the targeted biological systems, say a disease cell, at the destinations. The typically high affinity bond between the receptors and the ligands anchors the respective nanocarrier to the surface of the cells. We note that the process illustrated in Fig. 2(a) is typically nonlinear.

At this point the nanocarriers can be triggered to release the drug molecules in them. The released molecules diffuse across the extracellular space to the targeted cells, where they are received and processed. From the perspective of communication engineering, we can as well consider the nanocarrier as a transmitter, the extracellular space as a communication channel, and the targeted cells as the receivers, as is depicted in Fig.2(b). In this scenario, the released drug molecules are the information molecules that carry the molecular message meant for delivery to the targeted cells. Again, we note that the process illustrated in Fig. 2(b) is typically nonlinear.

Based on the above discussion, a precise knowledge of the characteristics of the delivery processes is required for accurate drug delivery. This implies that we have to be able to accurately predict the behavior of the transmitters, channels and receivers in the delivery process. However, in reality, the channels (vascular and extracellular) through which the nanoparticles (nanocarriers and drug molecules) traverse to reach their destinations are intrinsically random. More also, there may be some uncertainties in the transmitters (injection machine and nanocarriers) behavior as well as uncertainties in the responses of the receivers to signaling.

It is therefore required that irrespective of the complexity, nonlinearity, stochasticity, and multivariate characteristics, a set of given transmitted number of nanoparticles should elicit differentiated response at the receiver. By differentiated response we mean that the receiver should be able to respond over a dynamic range of possible transmitted signals. Typically, the sets of transmitted molecular signals primarily comprise molecular messages encoded in *type of molecules*, and *concentration of molecules* [5]. For the molecular-type encoding, the dynamic range of the differentiable responses is wide and depends on the number of the set of the complementary receptors on the targeted nanoreceiver. However, for concentration-type encoding the dynamic range of the differentiable responses is much smaller and depends significantly on the channel characteristics. Hence, our discussion is on the concentration dependent signalling.

If the distribution of the responses elicited by a weak molecular signal in a receiver overlaps with the distribution elicited by a stronger molecular signal, there is loss of information. For example, if the targeted disease cells cannot differentiate between two levels of the concentration of drug molecules, then we may be unable to accurate define dose-response curve for a given medication. The differentiability concern is particularly challenging to advanced TDD systems that depends on design protocols [20] to achieve seamless transmission among multiples nanosystems.

Therefore, analyzing the differentiability of the transmitted concentration-encoded molecular signaling, and the fidelity in molecular signal reception in the midst of system complexity, nonlinearity, stochasticity, and multivariate characteristics in a TDD system is at the heart of this work.

B. *Problem Definition*

In formulating the problem addressed by this work, we consider the inputs to the channel are defined based on some probability distributions that are mapped onto sets of probabilistic outputs at the receiver by a channel by some probabilistic distributions. The probabilistic distribution of the communication channel in the form of transition probabilities is obtained from stochastic simulation of the molecular channel, which takes into consideration the perceived, but approximated influences of the molecular channel. By using the probability distributions, we provide results of the mutual information measure. We also developed a relationship between mutual information and bioequivalent measure that differential drug delivery modalities.

III. Probabilistic System Model of TDD

Essentially, information-theoretic approach to system modeling starts by making statements about the probability distributions of the system. To establish intuition, we will present the probabilistic model of the TDD process in a modular format. The essential modules considered are the as those in Fig. 2, namely, the transmitter, the channel, and the receiver/destination.

A. *Transmitter Model of Targeted Drug Delivery System*

A given concentration level or concentration pattern carries a message. The message will usually be commands telling the intended receiver to respond by underdoing the desired chemical, physical and biological modifications. Regardless of the type of the message, what is common in the messaging is the presence or absence of certain concentration of the

signalling nanoparticles over a given time.

We shall let the transmitter output alphabet's symbols be the local concentration of the nanoparticles. Also, let A be the discrete random variable from the alphabet $\mathcal{A}$ comprising of M discrete level symbols, such that

$$\mathcal{A} = \{a_1, a_2, a_3, \ldots, a_M\} \quad (1)$$

For the sake of simplicity, we assume that $a_i < a_{i+1}$, which represent the various doses of the released nanoparticles. Further, we suppose that the transmitter emits the symbols a_i with the corresponding probability $P_{\mathcal{A}}(A)$ such that

$$P_{\mathcal{A}}(A) = \{p(a_1), p(a_2), p(a_3), \ldots, p(a_M)\} \quad (2)$$

Let us consider the case of a simple drug release from a nanocarrier loaded with specific drug molecules. When triggered by external stimuli, there is the possibility that the nanocarrier will release drug molecules or not with certain probability. A 'no release' implies a zero concentration, which we may assign a_1, and a 'release' indicates the transmission of a certain concentration, which we may assign a_4. There may be intermediate concentration levels that are associated with the uncertainty in the release process. In this sense, we let a_2 denote the concentration of nanoparticles undesirably released when 'no release' is actually intended. On the other hand, we let a_3 denote the concentration of nanoparticles undesirably emitted when the release 'a_4' is intended. The probabilities $p(a_i)$ depend on the efficiency of the trigger process. The same discussion applies to the injection machine mechanism.

The concentration of the transmitted molecules is usually influenced by uncertainties and the various factors inherent with the molecular propagation microenvironment [5]. Hence, the concentration of the molecules that diffuse to the reception location is always less than the initial concentration local to the transmitter. Therefore, it is imperative to say that the delivery process is designed to take care of this factor to ensure efficacious performance of the TDD system.

Just like in conventional electronic communication, the effect of the channel on the transmitted molecular signal can be corrected by an encoding process. Coding methods such as forward error correction (FEC) [21] and automatic repeat request have been widely employed in electronic communication. Some of these coding techniques have even be suggested for molecular communication [22], [23], [24]. However, it is important to take certain limitations of the MC nanosystems such as size, resources and technicalities into account before mapping techniques used in electronic communication directly to MC. Natural biological systems signaling such as the cell-to-cell signaling typically favor simplicity in design [25], hence, applying complex coding scheme to MC may not be appropriate as well as possible.

To buttress on the assertions we highlighted above with respect to the mapping of contemporary coding schemes to MC, let us consider the FEC. In electronic communication, the primary channel effects include attenuation, noise, delay spread, and frequency spread [26]. These effects results in the corruption of the transmitted message bits. Fundamentally, FEC-based channel coding involves the controlled addition of redundancy to a message sequence, which the receiver can use to check the consistence of the received bits. Hence, FEC-based channel coding entails the addition of extra redundant bits to the message sequence.

In the case of molecular signaling, we note that the channel effect in many instances can be anecdotally summed up under attenuation, delay (resulting in intersymbol interference (ISI)) and noise factors. A deeper discussion on the factors that influence molecules propagating in typical TDD microenvironment can be found in [5], [19]. To combat attenuation (and noise) the MC version of the FEC-based coding involves the addition of 'more molecules' (increased concentration), and to combat ISI, coding process involves the addition of 'more time' (duration before next transmission). Hence, a molecular channel encoder may simply operate as a *concentration encoder* or a *time encoder* as shown in Fig. 3.

The molecular channel coding function f_E is the mapping

$$f_E : \mathcal{A} \xrightarrow{f_E(t)} \mathcal{X}_i \quad (3)$$

where

$$\mathcal{X} = \{x_1, x_2, x_3, \ldots, x_M\} \quad (4)$$

We again suppose that the encoder emits the encoded symbols with the corresponding probability $P_{\mathcal{X}}(X)$ such that

$$P_{\mathcal{X}}(X) = \{p(x_1), p(x_2), p(x_3), \ldots, p(x_M)\} \quad (5)$$

In the simple nanocarrier release scenario, the concentration encoding process is usually predefined during the structural design of the nanocarrier and computation of the number of nanocarriers needed to combat the channel effect. The same applies to the injection procedure, where the concentration required to combat the channel impairment is pre-designed. The same applies to time encoding. However, in more complicated scenarios such as when using nanotransmitters that can synthesize drug molecules on demand, then the synthesis of the drug concentration level can be modulated by sensing the channel condition in feedback arrangement.

We note that like in all coding processes, extra resources are required at the transmitter to generate more molecules or time that are to be added to the original symbol. In this case, extra resources (energy/materials) are required at the transmitter for the encoding, which must be taken into account while designing the encoder. In this vein, we quantify the efficiency of a molecular encoder by the code factor Γ, which is equivalent to the code rate. Thus, increase in Γ implies that more resources are committed to the encoding process. This requirement places constraint on the use of complex encoding schemes for MC.

B. TDD Channel Model

The variable X whose value represents each of the encoded symbols is practically the concentration of nanoparticles emitted by the transmitter to represent an encoded symbol. Hence, it is this concentration X (considered deterministic and

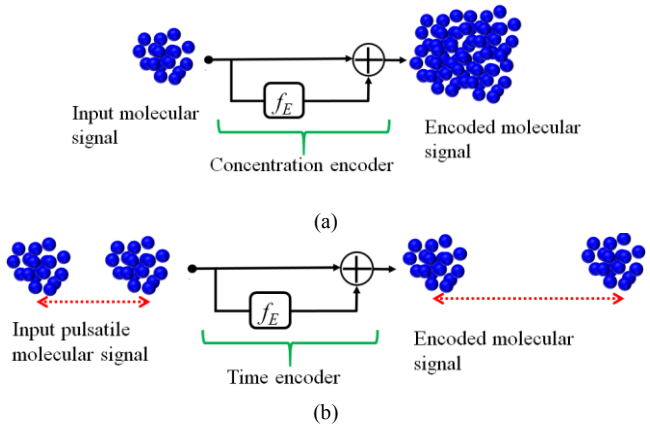

Fig. 3. The (a) concentration encoder and (b) time encoder for TDD.

equals to x_T at time $t = 0$) that diffuses through the channel to the receiver. The reaction-diffusion equation that governs the nanoparticle propagation can be expressed by

$$\frac{\partial X(r,t)}{\partial t} = \left\{\nabla.(D\nabla X(r,t)) - \nabla.(\vec{v}X(r,t)) - f(X)\right\}\Big|_{\partial\Omega} \quad (6)$$

with initial condition given by

$$X(r,0) = x_T\delta(r) \quad (7)$$

where $X(r, t)$ is the concentration of the nanoparticles at location r and time t, ∇ represents gradient, $\nabla.$ represents divergence, D is the diffusion coefficient of the medium, $\vec{v}$ is medium velocity, and $f(X)$ is the nanoparticle degradation function. The term indicates that X at $t = 0$ given by x_T is concentrated around some points on r such that $\int x_T\delta(r) \coloneqq x_T(t)$. The boundary conditions are defined on $\partial\Omega$. The factor $f(X)$ ensures that like in many natural nanoparticle signalling inside the body, the nanoparticles are degraded by enzymes and other processes [27].

Now, let the variable Y denote the fraction of X observed in a space V at the receiver location. Hence, f_{CH} is the channel mapping of X to Y, which include the mapping of the concentration of molecules to the number of molecules, thus

$$f_{CH} : \mathcal{X} \xrightarrow{f_{CH}(t)} \mathcal{Y} \quad (8)$$

where

$$\mathcal{Y} = \{y_1, y_2, y_3, \ldots, y_M\} \quad (9)$$

Accordingly, we can represent the probability of observing the variable Y in V with the corresponding marginal probability $P_{\mathcal{Y}}(Y)$ such that

$$P_{\mathcal{Y}}(Y) = \{p(y_1), p(y_2), p(y_3), \ldots, p(y_M)\} \quad (10)$$

With respect to Fig. 2(a), the space V is any of the targeted extracellular locations A, B and C for which the corresponding observation space is designated as V_A, V_B and V_C. In the case of Fig. 2(b) the space V is the conceptual volume space around a receptor on the targeted cell, if we assume molecular signal reception by means of ligand-receptor binding kinetics. This volume is assumed for each receptor and is defined by the distance between the receptor and the ligand, within which the ligand-receptor binding kinetics can only occur. Assuming we have Θ number of receptors on a targeted cell, then we have the corresponding V as $V_{R,\theta}$, $\theta = 1, 2, 3, \ldots, \Theta$.

The output probability $P_{\mathcal{Y}}(Y)$ of the channel is a function of the input probability $P_{\mathcal{X}}(X)$, the nanoparticle degradation factor $f(X)$, the microenvironment diffusion coefficient D, the dimension of the channel, $\partial\Omega$, the size of the reception space V and the time t of the observation. These factors are modelled by the *conditional probability* $P_{\mathcal{Y}\setminus\mathcal{X}}(Y\setminus X)$, which represent the probability that Y is observed in V given that X is released.

The number of nanoparticles Y_t observed in V at a given time instance t is a Poisson counting process. Since the counting operation happens in discrete time, we can denote the count at the index time $k = t/\Delta t$ by

$$Y_k \coloneqq \#\{X\big|_V\}\Big|_{t=k\Delta t} \quad (11)$$

$$Y = \sum_k Y_k, \quad 0 < k > K \quad (12)$$

where # stands for the cardinality of the set enclosed in the bracket and evaluated over the observation interval K.

To obtain $P_{\mathcal{Y}\setminus\mathcal{X}}(Y\setminus X)$ we present the hypothesis testing for $\mathcal{Y} = \{y_j\}$, given $\mathcal{X} = \{x_i\}$. We define Ξ_j as the number of nanoparticles whose range can be used to identify the corresponding symbols y_j. Since only a fraction of the nanoparticles concentration, $x_{T,i}$, $i = 1, 2, 3, .., M$ emitted at time $t = 0$ is observed in V, we can say that

$$\Xi_j = \gamma(X = x_{T,i}), \quad \forall i = j \quad (13)$$

where $0 \geq \gamma \leq 1$ is the fraction of the emitted nanoparticles that is observed in V. For instance, if we assign $\gamma = 0.007$ [28], then we expect that symbol x_1 is correctly received in, say in V, if about 0.7% of the transmitted nanoparticles is observed.

Let us consider $M = 4$, and assume that $x_1 < x_2 < x_3 < x_4$ and $y_1 < y_2 < y_3 < y_4$. We can formulate the hypothesis $H_j^{(y)}, j = 1,2,3,4$, for computing the probabilities of observing y_j in V given that x_i are sent, respectively, as follows:

$$H_1^{(y)}: \quad Y \leq \Xi_1 \quad (14)$$

$$H_2^{(y)}: \quad \Xi_1 < Y \leq \Xi_2 \quad (15)$$

$$H_3^{(y)}: \quad \Xi_2 < Y \leq \Xi_3 \quad (16)$$

$$H_4^{(y)}: \quad \Xi_3 < Y \leq \Xi_4 \quad (17)$$

Given that $x_{T,i}$ is transmitted, for N measurements of Y, we denote as F_i the set of Y realizations such that

$$F_i = \{Y_n^{(i)} : n = 1,2,3,\ldots,N\} \quad (18)$$

where is the $Y_n^{(i)}$ observed at nth measurement for a given input $x_{T,i}$. And let $G_{i,j}$ be the subset of F_i that satisfies $H_j^{(y)}$ such that

$$F_i = \bigcup_j^M \left(G_{i,j} \coloneqq F_i(H_j^{(y)})\right) \quad (19)$$

For example, let us as a matter of simplicity assume that for

$x_{T,3}$ = 80 molecules and N = 5, the set of Y observations are F_3 = {4, 7, 8, 2, 11} molecules. If $\Xi_1 = 0$, $\Xi_2 = 10$, $\Xi_3 = 20$ and $\Xi_4 = 80$, then $G_{3,1} := F_3(H_1^{(y)} = \{\}$, $G_{3,1} := F_3(H_1^{(y)} = \{4, 7, 8, 2\}$, $G_{3,1} := F_3(H_1^{(y)}) = \{11\}$ and $G_{3,1} := F_3(H_1^{(y)}) = \{\}$, which also satisfy (19).

We can therefore compute the conditional probability $P_{\mathcal{Y}\setminus\mathcal{X}}(Y \setminus X)$ from

$$P_{\mathcal{Y}\setminus\mathcal{X}}(Y \setminus X) := p_{ij}^{y}, \quad (i,j) \in \Re^{+} \tag{20}$$

where

$$p_{ij}^{y} := \frac{\#\{G_{i,j}\}}{\#\{F_i\}} = \frac{\#\{G_{i,j}\}}{N} \tag{21}$$

C. Received Molecular Signal Induction Model

As stated earlier, the number of nanoparticles observed in V is defined by Y, and is basically dependent on the channel characteristic as well as the volume of the reception space. However, the actual number of nanoparticles that is able to elicit response in the receiver is represented by the variable U. Hence, while Y represents the total number of molecules observed in V over T duration, U represents the number of nanocarriers that anchors in Fig.2a or the number of molecule-receptor binding that occurs in Fig.2b over the duration T. The relationships among X, Y and U are shown in Fig. 4.

The output alphabet $\mathcal{U}$ of the variable U is such that

$$\mathcal{U} = \{u_1, u_2, \ldots u_W\} \tag{22}$$

Accordingly, we can represent the probabilities of observing the alphabet $\mathcal{U}$ (the observable output alphabet of the TDD system presented in this work) with corresponding probability $P_{\mathcal{U}}(U)$ by

$$P_{\mathcal{U}}(U) = \{p(u_1), p(u_2), p(u_3), \ldots, p(u_W)\} \tag{23}$$

Hence, the mapping of Y to U is modelled by the *conditional probability* $P_{\mathcal{U}\setminus\mathcal{Y}}(U \setminus Y)$.

Whether we consider the scenario in Fig.2a or Fig. 2b, the transduction of Y to U is by the molecule-receptor binding process defined by the ligand-receptor binding kinetics, given by

$$L + R \underset{\xi_{-1}}{\overset{\xi_1}{\leftrightarrow}} LR \tag{24}$$

where LR is the molecule-receptor complex, ξ_1 is the forward reactions constant, and ξ_{-1} is the reverse reaction constant.

For Fig. 2a, while Y represents the number of nanocarriers that enter the space V_A, V_B or V_C, U represent the actual number that anchors at these spaces. The variable U depends on the number of anchorable points N_A in V, the probability of the ligands that are tethered to the nanocarriers to bind to the complementary receptor expressed at the targeted sites, and of course Y [8]. With the typical high affinity ligand-receptor binding associated with this scenario, we simply assume that any nanocarrier that enters V_A, V_B and V_C, will anchor at the sites until all the anchorable points are occupied. Therefore, U depends only on N_A and Y. We can further simplify things by assuming that N_A is very large, in this case, Y is approximately proportional to U.

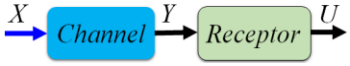

Fig. 4. Block diagram of the transmit-receive model for the TDD scenario.

For Fig. 2b, the conceptualized reception space V_R represents the radial separation distance between a receptor and a diffusing drug molecule within which binding may only occur. Hence, while Y represents the number of the emitted drug molecules that enter the space V_R, U represents the eventually number that initiates the ligand-receptor binding. In this case, the variable U depends on the probability of the drug molecule-receptor binding, and of course, Y.

To compute U for Fig. 2b, let the probability that a ligand at kth interval on Y binds to a receptor is given by

$$p_{R,k} = Y_k (k_d + Y_k)^{-1} \tag{25}$$

$$k_d = \Lambda_{\max} \Phi e^{\frac{\Delta\varepsilon}{K_B T_0}} \tag{26}$$

where k_d is the ligand-receptor reaction dissociation constant. The symbol $\Lambda_{\max}$ is the maximum number of molecules that can fit into V_R; Φ is the molar mass of the signalling molecule; $\Delta\varepsilon$ is the difference between the free ligand energy and the energy when bonded to a receptor; K_B is the Boltzmann constant; and T_0 is the medium temperature in Kelvin.

Therefore, for a given input $x_{T,i}$, the probability of φ successful molecule-receptor binding over K sample times can be model as a Poisson-binomial distribution with variable probability function $P_{R,k}$, thus

$$\beta^{(i)}(K = \varphi) = \sum_{Q \in B_\varphi} \prod_{k \in Q} p_{R,k} \prod_{v \in Q^c} (1 - p_{R,v}) \tag{27}$$

where B_φ is defined as the set of all subsets of size φ that can be chosen from the set {1, 2,…, K}, Q^c is the complement of Q (i.e., Q^c = {1, 2,…, K} \ Q).

If we consider only the set of all Y_k with values greater than zero, we can define the following ordered set

$$Y_l = \{Y_k \neq 0 : l = 1,2,3,\ldots,L, \; L \leq K\} \tag{28}$$

where the probability of binding for the set is $\{p_{R,l}\}$. Hence, for relatively small V, we can approximate (27) to a binomial distribution, thus

$$\beta^{(i)}(L = l) = \binom{L+1}{l} p_R{}^{l} (1 - p_R)^{(L+1)-l} \tag{29}$$

where p_R is the average value of $p_{R,l}$.

Therefore, to obtained the probabilities of binding that define u_1, u_2, u_3 and u_4 from (29), we define the following hypothesis for the variable U.

$$H_1^u: \quad \Gamma_1 < U \leq \Gamma_2 \tag{30}$$

$$H_2^u: \quad \Gamma_2 < U \leq \Gamma_3 \tag{31}$$

$$H_3^u: \quad \Gamma_3 < U \le \Gamma_4 \tag{32}$$

$$H_4^u: \quad \Gamma_4 < U \ge \Gamma_5 \tag{33}$$

where $\Gamma_1, \Gamma_2, \Gamma_3, \Gamma_4$ and Γ_5 defines the range of the number of successful molecule-receptor binding that identifies, u_1, u_2, u_3 and u_4.

Hence, for a given input $x_{T,i}$,

$$\alpha_{j,i} := \beta^{(i)}(H_i^u) = \begin{cases} \sum_{l=\Gamma_i}^{\Gamma_{i+1}} \beta^{(i)}(L=l), & L \ge \Gamma_i \\ 0, & otherwise \end{cases} \tag{34}$$

conditional on

$$\sum_{w=0} \alpha_{j,i} = 1 \tag{35}$$

Consequently, the conditional probability $P_{U\backslash Y}(U \setminus Y)$ can be computed from

$$P_{U\backslash Y}(U \setminus Y) := \alpha_{j,i}, \quad (i,j) \in \Re^+ \tag{36}$$

For N sets of observations $\alpha_{j,i}$ can be obtained by averaging L and p_R over all N realizations, and using the averages to compute (29), and subsequently, (36).

IV. Practical Realization of the TDD Channel Model

To be able to compute the conditional probabilities in (20) and (36), which are not known a priori but have to be measured experimentally [29], the realization of (12), which is achieved by solving (6), is required. We shall discuss the numerical and stochastic methods used in this work to solve (6) for Fig. 2a and 2b, respectively.

A. Injection Machine –to-Targeted Site Channel Model Realization

We approach the realization of (6) using the popular pharmacokinetic compartmental model. The pharmacokinetic compartmental model illustrated in Fig. 5 is often used to model the course of the nanoparticles from the point of injection to the targeted sites [8]. In employing this model the following assumptions are made. 1) The rate of nanoparticles movement between compartments obeys a first-order reaction law. 2) The nanocarriers are homogeneously distribution within the compartments. 3) The space V_A, V_B and V_C do not vary with time. 5) The nanoparticles are completely eliminated from the body through the blood compartment.

The central compartment V_α, is the blood circulatory system with concentration of nanocarriers designated by $y_\alpha(t)$.The concentration of the nanocarrier in each compartment that represents the targeted sites V_A, V_B and V_C is given by y_A, y_B and y_C, respectively. The function $y_a(t)$, $y_b(t)$ and $y_c(t)$ are the concentrations of the nanoparticles that anchor at the sites A, B, and C, respectively. The function $y_{el}(t)$ is the concentration of the eliminated nanoparticles as a function of the elimination rate k_{el}., which accounts for all the loss in concentration of the nanocarriers. The parameters $k_{\alpha A}$, k_{Aa}, $k_{\alpha B}$, $k_{B\alpha}$, $k_{\alpha C}$, and $k_{C\alpha}$ are

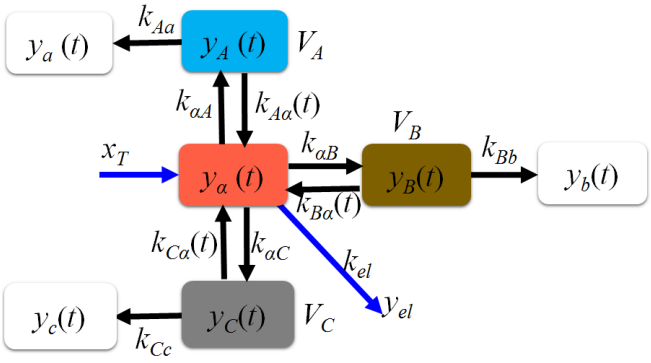

Fig. 5. Multi-compartmental model for nanocarrier propagation to targeted site.

first-order rate constant in and out of the compartments. These rate constants are typically dependent on the concentration difference between the compartments, the size of the fenestra leading to the sites, and the properties of the diffusing molecules. The parameters k_{Aa}, k_{Bb}, and k_{Cc} are the rate constants of anchoring at each of the targeted site.

On entering the spaces V_A, V_B and V_C, the nanocarriers bind to the complementary receptors at these targeted destinations with high affinity bond. This implies that the dissociation constant for the binding is approximately zero; hence, the probability of a nanocarrier anchoring on a receptor depends only on the number of free ligands on the nanocarrier and the unbounded receptors at the targeted site.

Let us assume that the concentration of the receptors that each nanocarrier can bind to at each targeted site is $N_{R,i}(t), i \in \{a,b,c\}$, and the injected concentration of the nanocarrier is x_T/V_α. Consequently, the pharmacokinetic process in Fig. 5 can be described by the following differential equations

$$\frac{dy_\alpha}{dt} = -[k_{\alpha A}y_\alpha(t) + k_{\alpha B}y_\alpha(t) + k_{\alpha C}y_\alpha(t)] + [(k_{A\alpha}y_A(t) + k_{B\alpha}y_B(t) + k_{C\alpha}y_C(t))] - k_{el}y_\alpha(t) \tag{37}$$

$$\frac{dy_A}{dt} = -k_{\alpha A}y_\alpha(t) - k_{Aa}y_A(t) + k_{A\alpha}y_A(t) \tag{38}$$

$$\frac{dy_B}{dt} = -k_{\alpha B}y_\alpha(t) - k_{Bb}y_B(t) + k_{B\alpha}y_B(t) \tag{39}$$

$$\frac{dy_C}{dt} = -k_{\alpha C}y_\alpha(t) - k_{Cc}y_C(t) + k_{C\alpha}y_C(t) \tag{40}$$

$$\frac{dy_a}{dt} = k_{Aa}y_A(t)N_{Ra}(t) \tag{41}$$

$$\frac{dy_b}{dt} = k_{Bb}y_B(t)N_{Rb}(t) \tag{42}$$

$$\frac{dy_c}{dt} = k_{Cc}y_C(t)N_{Rc}(t) \tag{43}$$

with the initial conditions $y_\alpha(0) = x_T/V_\alpha$, $y_A(0) = y_B(0) = y_C(0) = y_a(0) = y_b(0) = y_c(0) = 0$, and $N_{R,a}(0) = N_{R,a}$, $N_{R,b}(0) = N_{R,b}$ and $N_{R,c}(0) = N_{R,c}$. In this work, the solution to (37)-(43) is obtained using the 4th-order Runge-Kutta numerical method.

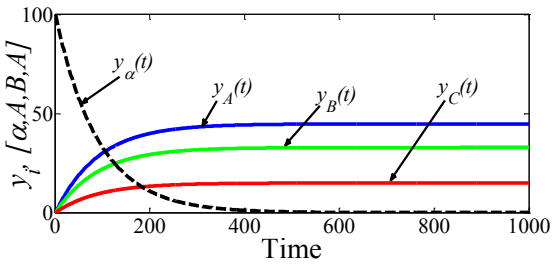

Fig. 6. Plot of $y_i(t)$, $i = \{\alpha, A, B, C\}$ vs time.

When the parameters k_{Aa}, k_{Bb}, and k_{Cc} are set to zero, the peak values of $y_A(t)$, $y_B(t)$ and $y_C(t)$ define Y for the sites V_A, V_B and V_C , respectively. Where the parameters k_{Aa}, k_{Bb}, and k_{Cc} are not set to zero, the peak values of $y_a(t)$, $y_b(t)$ and $y_c(t)$ define U for the sites V_A, V_B and V_C , respectively. A sample of the output of the pharmacokinetic model is shown in Fig.6.

We note that in the pharmacokinetic models presented here, the only channel effect considered is the degradation/ elimination factor. There are other models such as those that are based on the diffusion phenomenon [30] that can be employed. However, for very accurate representation, the various channel effects such as those enumerated in [5] have to be considered in such models to obtain more accurate model and resultantly better estimation of the channel output.

B. Nanocarrier -to-Targeted Cell Channel Model Realization

To realize (6) for the scenario in Fig. 2(b), we employ the 2D lattice-based diffusion simulation model [31] depicted in Fig.7. To this end, the following considerations are made.

i. The communication microenvironment $\Omega \in \{V_A, V_B, V_C\}$ is bounded by $\partial\Omega$ with length H_L and width H_W. It is divided into voxels, where for sample time Δt the square dimension of the voxel is calculated from

$$d_{vox} = \sqrt{4\pi D \Delta t} \tag{44}$$

ii. The dynamics of the emitted drug molecules are according to the principle of Brownian motion, and their diffusion coefficient is D. Factors such as the drag effect, which is a function of the medium velocity [32], are not considered here since the velocity of the extracellular medium is very low.

iii. Only one molecule can occupy a voxel at any time.

iv. We consider a single spherical nanocarrier of radius r_X, and a targeted cell of radius r_R; both are fixed at r distance from each other within Ω.

v. We focus on the signalling mechanism of ligand-receptor binding that initiates *second messenger* signalling in a cell. And we consider the communication with only a single receptor on the targeted cell.

vi. A conceptualized reception space V_R around the receptor within which the reaction in (24) occurs at a given time instant. We express the number of voxels L_{vox} that define this space V_R as

$$L_{vox} = \left| (r_M + r_P + r_F) d_{vox}^{-1} \right| \tag{45}$$

where r_M is the radius of the molecules, r_P is the radius of the receptor active site, and r_F is the radius of the intermolecular attraction between the information molecule and the receptor.

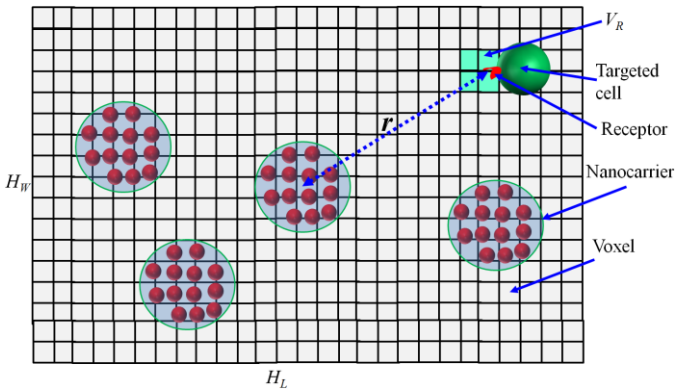

Fig. 7. 2D lattice-based molecule diffusion simulation model.

vii. The emitted molecules are degraded at the rate constant k_d.

viii. The number of molecules observed in V_R defines Y.

V. Molecular Information and Uncertainty

As a recap, the aim of employing information theory in MC analysis is to afford us a way of analysing the MC system irrespective of its complexity. Specifically, we want to be able to 1) analyse the uniqueness of the encoded symbols, and, 2) quantify the efficiency with which the diffusion channel and the receptor-ligand process maps the variable X to Y (or U). Information theoretic measures such as *entropies* and *mutual information* can be employed to address these objectives.

A. Entropy

The entropy of a system represents the amount of uncertainty *one particular observer* has about the state of the system. For instance, if we consider the observation made particularly on the transmitter, where the encoded alphabet is $\mathcal{X}$ with probability $P_{\mathcal{X}}(X)$, then the entropy H of say a random variable X is given by Shannon's formula

$$H(X) = -\sum_{x_i \in \mathcal{X}} p(x_i) \log_2 p(x_i) \geq 0 \tag{46}$$

Following (46), we can also express $H(Y)$, and $H(U)$ as Shannon's formulas.

The expression in (46) may provide us with a way of quantifying the efficiency of, for instance, a transmitter. As an example, let us assume that we have theoretically designed a nanocarrier to emit no molecule (designated the symbol x_1) at the absence of a trigger, and to emit certain concentration of molecules (designated the symbol x_4) when triggered by an external stimulus. We further assume that the probabilities of emitting x_1 and x_4 are equal. Hence, using 'b' equal to 2, the entropy is 1 bit. Let us assume that on fabricating and testing the nanocarrier, we observe that in addition to emitting symbols x_1 and x_4, extra intermediate symbols x_2 and x_3 are possible as a function of the system error. Assuming a uniform probability for x_1, x_2, x_3 and x_4, the entropy is 2 bits.

This tells us that there is more uncertainty about our practical transmitter compared to the theoretical transmitter. Obviously, by lowering the probability of say x_2 and x_3 we can reduce this uncertainty.

B. Joint Entropy

In information theory, we can quantify the uncertainty associated with two variables using the *joint entropy*. If we consider the pair of discrete random variables (X, Y) with joint probability $p(x_i, y_i)$, the joint entropy is expressed as

$$H(X,Y) = -\sum_{x_i \in \mathcal{X}} \sum_{y_i \in \mathcal{Y}} p(x_i, y_i) \log_b p(x_i, y_i) \tag{47}$$

If X and Y are independent, then

$$H(X,Y) = H(X) + H(Y) \tag{48}$$

The usefulness of the joint entropy measure in MC analysis can be seen in quantifying the influence of two or more signalling pathways that must work together to produce a response at the receiver. For instance, let us assume that a certain pathway designated as P_{w1} has to work with another pathway P_{w2}, to produce a certain response in the targeted cell. If there is a set of candidate pathways whose elements can be combined in different ways to form P_{w2}, then the joint entropy measure of each of the combination options and P_{w1} can help us choose the P_{w2} that ensures that the uncertainty obtained by observing P_{w1} and P_{w2} simultaneously, is minimized. This is invariably one of the objectives of drug discovery, especially for drug combination therapy.

C. Conditional Entropy

The entropy of the molecular channel output Y given that we know something about the channel input X is termed conditional entropy. The conditional entropy is defined as

$$H(Y \setminus X) = -\sum_{x_i \in \mathcal{X}} \sum_{y_i \in \mathcal{Y}} p(y_i \setminus x_i) \log_b p(y_i \setminus x_i) \tag{49}$$

where $P_{\mathcal{Y} \setminus \mathcal{X}}$ $(Y \setminus X)$ = $p(y_i \setminus x_i)$ is the conditional probability expressed by

$$p(y_i \setminus x_i) = \frac{p(x_i, y_i)}{p(x_i)} \tag{50}$$

The output probability $p(y_i)$ can be obtain from (50) by

$$p(y_i) = \sum_{x_i \in \mathcal{X}} p(x_i, y_i) = \sum_{x_i \in \mathcal{X}} p(y_i \setminus x_i) p(x_i) \tag{51}$$

The usefulness of the conditional entropy measure to TDD analysis can as well be seen in quantifying the influence of two or more signalling pathways that must work together to produce a response at the receiver, as described for joint entropy. However in this case, in respect to drug discovery, it is assumed that we have good knowledge of a primary target pathway, say, P_{w0} and the complementary target drug molecule. The use of conditional entropy helps us to evaluate the uncertainty in the sets of the pathways and lead molecules that will work with P_{w0}.

VI. Mutual Information

Regardless of the underlying physical basis or complexity of any molecular channel or any communication channel for that matter, the channel can be reduced to a "black box" that maps an input onto an output. Hence, the molecular channel and the receptor channel in Fig. 4 can be considered as 'black boxes' with input X mapped to output Y, and channel output Y mapped to U, respectively. Consequently, one of the main goals of any communication is to determine from Y (or as the case may be, U) what information is contained in X (or Y).

A. Mutual Information as a Measure of Molecular Signalling Fidelity and Differentiated Response

As we pointed out before, the entire TDD system is often nonlinear. Hence, we need a measure that quantifies the amount of information that the value of one random variable contains about the value of another random variable, given that the communication channel is characteristically nonlinear, complex, and multivariate. An information theoretic measure that is often employed for this task is the mutual information (MI), which is always symmetric and nonnegative. Indeed, the MI is arguably the best measure of correlation between two random variables when the underlying relationship is nonlinear [33]. The MI between two variables, say, the variable X and the output variable Y is expressed as

$$I(X;Y) = H(X) - H(X \setminus Y) \tag{52}$$

and in relation to the joint distribution and the product distribution of X and Y, it is given by

$$I(X;Y) = -\sum_{x \in \mathcal{X}} \sum_{y \in \mathcal{Y}} p(x,y) \log_b \frac{p(x,y)}{p(x)p(y)} \tag{53}$$

At the point when the output has not yet been observed, the computation of the MI using (53) is not possible. In this case, if we have some knowledge of the channel probability, then we can express the MI as a function of the channel and input probabilities by substituting (50) and (51) into (53), to yield

$$I(X;Y) = -\sum_{x \in \mathcal{X}} \sum_{y \in \mathcal{Y}} p(x_i) p(y_i \setminus x_i) \log_b \frac{p(y_i \setminus x_i)}{\sum_{x_i \in \mathcal{X}} p(y_i \setminus x_i) p(x_i)} \tag{54}$$

Hence, given that we know $p(x_i)$, by computing (20) and (36) we can obtain the measures in (46), (47), (49) and (54). For a molecular channel, we will expect that $I(X;Y) \rightarrow 0$; hence, the fidelity of the signaling process is gradually lost as $I(X;Y) \rightarrow 0$. This simply means that the uncertainty in the channel overwhelms the transmitter uncertainty. To improve on the MI, we must reduce channel uncertainty, maybe by changing delivery routes to a one with lower entropy or modify the signaling molecules and symbols to militate against the channel uncertainty. As the channel gets very good, $I(X;Y) \rightarrow H(X)$, which that the uncertainty in the channel becomes insignificant compared to the transmitter uncertainty. Obviously, signaling fidelity is directly proportional to the

differentiability of the signaling process. Note that in the models presented in this paper and simplified in Fig. 4, (46)-(54) represents the TDD system input-output relationship when we consider only the transmitter-to-channel output (input of receiver) is considered. With Y and U replacing X and Y, respectively, in (46)-(54), the channel output-to-receiver output relationship is considered. In the case where X and U replacing X and Y, respectively, in (46)-(54), the end-to-end (transmitter-to-receiver) relationship is considered.

B. Mutual Information as a Measure of Bioequivalence

Bioequivalence [34] is an important measure in TDD that shows the therapeutic equivalence of two or more different formulations or administration modes. The MI metric can be used to ascertain the relativeness of two or more nanocarrier designs or the administration modalities for nanocarriers in a TDD system. This is so since, like correlation function, MI is known to be a powerful tool to characterize the correlations among systems, especially systems of numerical and symbolic sequences [35].

Let us consider, say, the information exchange between two different nanocarriers Q and S and a receiver relative to the same molecular channel. We assume that the nanocarrier Q is the reference nanocarrier with ideal output; hence, it is our reference system. We propose that the difference between their MIs $I_Q(X;Y)$ and $I_S(X;Y)$ is a measure of their bioequivalence, $\Delta I(X;Y)$. This proposition is intuitive from the expression of MI (52). The difference in MI is given by

$$I_{S-Q}(X;Y) = \underbrace{\left(H_S(X) - H_Q(X)\right)}_{TX} - \underbrace{\left(H_S(X \setminus Y) - H_Q(X \setminus Y)\right)}_{ChXY} \tag{55}$$

where TX is the MI contribution due to the transmitter uncertainty, and $ChXY$ is the MI contribution due to the channel uncertainty.

Since we are considering the same channel of information transfer, $ChXY$ is a function of the variance of the channel's probability distribution. Assuming channel reciprocity, if the variance is negligible, like in a noiseless channel, then $H_Q(X/Y) = H_S(X/Y)$, so that

$$\Delta I(X;Y) = H_S(X) - H_Q(X) \tag{56}$$

Hence, in this situation, the bioequivalence is simply a function of the nanocarriers' entropies. When $\Delta I(X;Y)$ is zero, there is a perfect equivalence between the two systems. The bioequivalence reduces as $\Delta I(X;Y)$ deviates from zero. And the sign of $\Delta I(X;Y)$provides us with the information on which of entropies $H_S(X)$ and $H_Q(X)$ contributes to the $\Delta I(X;Y)$ deviation from zero. As can be deduced from (56), when $\Delta I(X;Y)$is greater than zero, it implies that the deviation from perfect equivalence is due to the variation in the transmitter uncertainty, $H_S(X)$. And when $\Delta I(X;Y)$is less than zero, it implies that the deviation from perfect equivalence is due to variation in channel uncertainty, $H_Q(X)$.

On the other hand, let us consider that the entropy of Q and S are the same (similar nanocarriers), but they signal the same receiver on different molecular channels. Hence, the bioequivalence is simply a function of the channel entropies. Following (55), as $\Delta I(X;Y)$ goes negative it implies that the channel experiences by S is much bad compared to that of the reference system.

As an example, let us assume that $H_S(X)$ = 0.8 bit and $H_Q(X)$ = 1.0 bit. If the both transmitter, namely, S and Q, transmit to a targeted site through the same channel, then considering (55), $\Delta I(X;Y)$ = -0.3. This implies that both delivery systems are not equivalent, and that there is more uncertainty in Q than in S transmitter output. If S and Q transmit through different channels each with $H_S(X\setminus Y)$ = 0.4 bit and $H_Q(X/Y)$ = 0.3 bit, respectively, then, $\Delta I(X;Y)$ = -0.3. This implies that the bioequivalence of the two systems is modified to being closer by the difference in their channels' uncertainties.

VII. Numerical Results and Discussion

In this section, we carry out some simulation to explore the information-theoretic approach to MC in general and TDD in particular. Measures such as the MI and its subset the bioequivalence are considered in the evaluation of the TDD process. Firstly, we lay out the experimental scenarios and parameters for the simulation of each of the modules, namely, transmitter, channel and receiver. Then, we present the simulation results and discussions of the information-theoretic measures for the X-Y systems (transmitter-to-reception space) and the X-U systems (transmitter-to-receptor output).

A. Experimental Design of the Simulation Scenarios

Transmitter Parameters

For Fig. 2a, to set the values of the input alphabet, we consider the clinical intravenous injection errors due to wrong dose administration. This could be error due to human oversight and inefficiency or due to the injection machine inefficiency. A conventional 10ml syringe has the capacity of injecting over 3 billion nanocarriers of 100 nm radius in a single shot [8]. In this work, for ease of computation, we scale down the maximum number nanocarriers injectable to about 10000. We assume that based on some test results, we approximately assign the elements of the encode output alphabet of the injection machine the dimensionless values x_1 = 0 (for no injection), x_2 = 500 (error due to machine fault when x_1 is intended), x_3 = 5000 (error due to medical personnel fault when x_4 is intended) , and x_4 = 10000 (for full dose), with probabilities $p(x_1)$, $p(x_2)$, $p(x_3)$ and $p(x_4)$. For five different tests cases, namely, **Case 1** to **Case 5**, these probabilities are arbitrarily chosen and are given in Table I. While the probability values are arbitrarily chosen, a trend can be observed in the table that indicates the assumed bias towards on kind of error or the other.

In the case of Fig. 2b, let us consider a drug-encapsulating liposome as the nanocarrier. We assume that the nanocarrier is of radius 100 nm and encapsulates doxorubicin molecules [36]. The radius of $r_M \leq 5.0\times10^{-9}$ m is chosen for the drug

molecules, which is typical for small molecules. This implies that for $r_M = 5.0\times10^{-9}$ m a 100 nm radius nanocarrier can carry 8000 molecules. However, for ease of computation, we scale down the maximum number molecules carried by a nanocarrier to about 200. Let us further assume that the nanocarrier is fabricated using three different technologies/methods, for which we designate each set by Liposome *A*, Liposome *B* and Liposome *C*. We arbitrarily take it that on being triggered by external stimuli, the nanocarrier ideally releases about 200 molecules, but emits none when not triggered. Let the practical tests carried out on each set of the nanocarriers indicate some departure from the ideal scenario. Hence, on being triggered, about 200 molecules are releases at some instants, but in other instants an average of 150 molecules are released. And when the nanocarrier is not on trigger, no molecule is released at some instants, but in other instants, an average of 50 molecules is undesirably released. The assumption here is that the output of the nanocarrier is the encoded message. Based on the average result of the tests, we approximately assign the elements of the encode output alphabet of the nanocarrier the values $x_1 = 0$, $x_2 = 50$, $x_3 = 150$, and $x_4 = 200$, with probabilities $p(x_1)$, $p(x_2)$, $p(x_3)$ and $p(x_4)$, respectively. The output probabilities of each set of the nanocarrier, which is chosen arbitrarily, are given in Table II. However, while the probability values are arbitrarily chosen, a trend can be observed in the table that indicates the assumed bias towards one type of error or the other.

TABLE I
OUTPUT PROBABILITIES OF THE INJECTION MACHINE

	$p(x_1)$	$p(x_2)$	$p(x_3)$	$p(x_4)$
Case 1	0.5	0	0	0.5
Case 2	0.4	0.1	0	0.5
Case 3	0.25	0.25	0	0.5
Case 4	0.5	0	0.1	0.4
Case 5	0.5	0	0.25	0.25

TABLE II
OUTPUT PROBABILITIES OF THE NANOCARRIERS

	$p(x_1)$	$p(x_2)$	$p(x_3)$	$p(x_4)$
Liposome A	0.5	0	0	0.5
Liposome B	0.4	0.1	0	0.5
Liposome C	0.25	0.25	0	0.5
Liposome D	0.5	0	0.1	0.4
Liposome E	0.5	0	0.25	0.25

Molecular Channel Parameters

For the scenario in Fig. 2a, the resulting first-order ordinary differential equations are solved numerically using numerical method. Based on the results from [37], [38], for the pharmacokinetic of liposome-based nanocarriers in oncology, the following values; $k_{el} = 0.0082$ min^{-1}, $k_{A\alpha} = 0.00125$ min^{-1}, $k_{\alpha B} = 0.0367$ min^{-1}, $k_{B\alpha} = 0.0124$ min^{-1}, $k_{\alpha C} = 0.0167$ min^{-1} and $k_{C\alpha} = 0.0044$ min^{-1} are used in the simulations. For the analysis of the MI, we concentrate on *Site A* and evaluate the system performance for the variation in $k_{\alpha A}$ across the range of 0 to 0.1 min^{-1}. The variation in $k_{\alpha A}$ indicates how open the fenestration at the *Site A* is. Hence, the higher the values of $k_{\alpha A}$, the more open the fenestra. For the scenario in Fig. 2b, we consider transmission from a nanocarrier at different distances r from the targeted cells. For simplicity, the dimension of the microenvironment is considered to extend to infinity.

The simulation time step is set to 0.01 μs. The value of the diffusion coefficient D is taken to be 1.0×10^{-6} cm^{2}s^{-1} [39]. As mentioned earlier, the radius of $r_M \leq 5.0\times10^{-9}$ m is chosen for the drug molecules, where for doxorubicin molecules the radius is about 1.5×10^{-9} m [40]. The radius of the receptor active site is chosen to be 8×10^{-9} m [41]. We consider the intermolecular force distance r_F to be 2.9×10^{-10} m [42]. Hence, by using the values of r_M, r_P and r_F, the value of r_S and subsequently, L_{vox}, can be obtained from (8). The degradation constants used are specified for each of the results obtained.

Nanoreceiver Parameters

For the receiver in Fig. 2a, we consider that the concentration of the nanocarriers that can anchor at V_A, V_B and V_C are N_{Ra}, N_{Rb} and N_{Rc}, respectively, where $N_{Ra} = N_{Rb} = N_{Rc} = 2500$. We assume that about 20% of the transmitted nanoparticles concentration reliably defines the channel outputs such that the dimensionless designations $y_1 = 0$, $y_2 = 0 < Y < 100$, $y_3 = 100 < Y < 2000$, and $y_4 = 2000 \leq Y$, hold. The choice of the output percentage can be defined by the nanoparticles concentration that achieves therapeutic results. In this work, given that contemporary nanoparticle delivery systems recorded an average of about 1% [28], we have arbitrarily scales this up by a factor of 20 in lieu of the maximum releasable molecules.

For the receiver in Fig. 2b, we consider that the molecules released by a nanocarrier that is r distance from the nanoreceiver, targets a receptor on the nanoreceiver. Again, we assume that about 20 % of the transmitted nanoparticles genuinely defines the channel outputs such that $y_1 = 0$, $y_2 = 0 < Y \leq 20$, $y_3 = 20 < Y \leq 39$, and $y_4 = Y > 39$. The molar mass of $\Phi = 543.52$ g/mol for doxorubicin is used.

B. Mutual Information Test for TDD Efficiency and Bioequivalence

Figure 8 shows the change in MI (for the *X-U* system) as a function of the size of the fenestrae represented by the variation in $k_{\alpha A}$ for the scenario where the probability of erroneous dose delivery is due to uncertainty in the injection machine. Implicitly, Fig. 8 compares the MI for Case 1 Case 2 and Case 3. And in Fig. 9 the change in MI as a function $k_{\alpha A}$ for the scenario where the probability of erroneous dose delivery due to the uncertainty in the medical personnel procedure is shown. Implicitly the MI comparison is among Case 1, Case 4 and Case 5.

It can be seen from Fig. 8 and 9 that as $k_{\alpha A}$ increases, the MI increases, indicating that more information about the transmitted molecular signal is received at the destination. That is to say that better delivery of the desired dose of nanocarriers to the targeted site is achieved with a more open fenestra. However, the MI saturates at some values of $k_{\alpha A}$ such that there is no more increase in the delivery efficiency even with large fenestra.

The MI also affords us a way of identifying and differentiating the impact of the transmitter error from the molecular channel uncertainty in the TDD process. This is easy to verify from (52) by quantifying the contribution of the input entropy $H(X)$ and the reverse channel entropy $H(X\backslash Y)$. Firstly, we identify the target MI, which is the 'best' MI that represents the ideal scenario where input entropy is ideal, and the channel entropy is at the lowest. For this best MI is at 1 bit. Hence, any MI value above the target MI is considered to be due to the contribution from erroneous behavior of the transmitter. On the other hand, MI values below the target MI is due to the contribution from the uncertainty in the molecular channel.

The MI analysis can be employed to know the ability of the TDD process to discriminate or differentiate between two levels of the transmitted symbols. In Fig. 10, we exemplify this by considering the discriminability of x_3 and x_4 at the receiver. For example, for Case 5, we kept x_4 at 10000 and vary x_3 as 1000, 5000 and 8000. It can be seen that as the difference between the levels of the symbols increases, the ability of the system to differentiate between the symbols increases. For instance, Fig. 10 shows that the pair (x_4 = 10000 and x_3 = 1000) is more discriminable than (x_4 = 10000 and x_3 = 8000.). The level of the differential response can easily be quantified by comparing the distance between the MI of the target MI and each of the symbol pairs under consideration.

For Fig. 2b, we analyse and compare the information-theoretic measures of the output characteristics of the molecular channel, which includes the diffusion molecular channel and the ligand-receptor channel. In Fig.11-19, the MI and bioequivalent measures of the scenarios defined in Table II are presented in the case of the diffusion molecular channel, where the output variable is Y, and the ligand-receptor channel, where the output variable is U. In Fig.11a, for the X-Y system, the MI as a function of distance r is presented to evaluate the effect of the nanocarrier error due to *false stimulation* (Liposome A, B and C) at k_d = 0.0033 min^{-1}. And in Fig.1b, for X-Y system and k_d = 0.0033 min^{-1}, the MI as a function of distance r is presented to evaluate the effect of the nanocarrier error due to *inadequate release* (Liposome A, D and E). It can be seen from Fig. 11a and Fig.11b that the MI decreases with distance, which is expected since the channel uncertainty increases with distance.

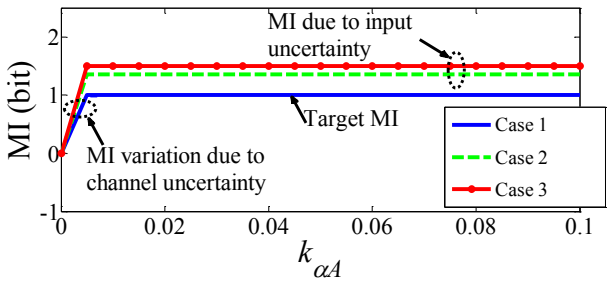

Fig. 8. Mutual information variation with channel degradation for the communication system between the injection machine and the targeted extracellular space, where there is error due to injection machine imperfection.

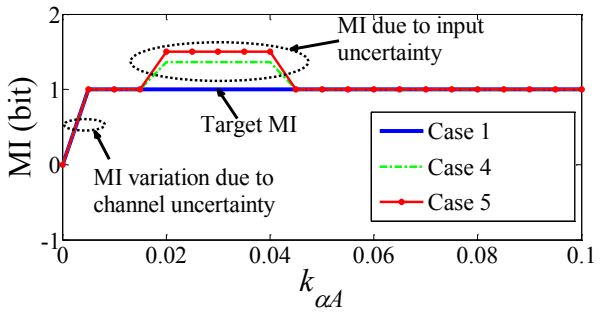

Fig. 9. Mutual information variation with channel degradation for the communication system between the injection machine and the targeted extracellular space, where there is error due to medical personnel oversight.

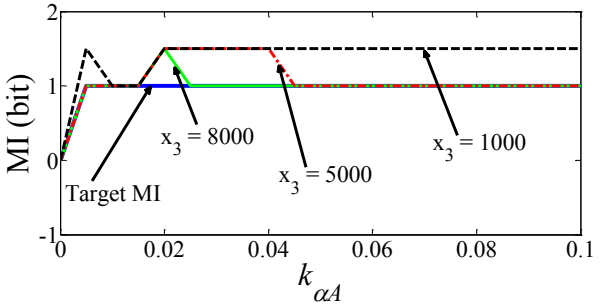

Fig. 10. Discriminability of the injection machine-targeted extracellular space system as a function of input signal range and channel degradation factor.

The differentiability of the input alphabet $\mathcal{X}$ is decipherable from the MI graph in Fig. 11a and 11b. As MI reduces, the possibility of obtaining differential response reduces. For instance, for the input probability distribution in Liposome A, B and C, the maximum values of MI, which indicate perfect differentiated response, are 1 bit, 1.36 bit and 1.5 bit, respectively. In Fig. 11a, while the input alphabet of Liposome A is differentiable at the receiver (since MI is at its maximum of 1 bit) over some distance, there is significant loss in the differentiability of the input alphabet of Liposome B and C at the receiver (since their MIs are lower that their maximum) over all distances. From Fig. 11b, the differentiability of the input alphabet of Liposome E follows the same argument as in Fig. 11a with Liposome D and E being a little more differentiable in Fig. 11b than in Fig. 11a. The implication of these observations is that for the scenarios in Table II, assuming that the input alphabet are valid message symbols, then signalling over the channel under consideration will present considerable errors, which increase with distance. However, we note that we have only considered this analysis to the point of the ligand-receptor binding process. The inclusion of typical biological circuitry of the targeted cell is not taken into consideration, which gives, if considered, the end-to-end MI.

In Fig.12a and Fig.12b, the effects of the signal induction process of the ligand-receptor binding on the TDD signalling are shown. All the arguments that arise in Fig. 11a and b are directly extendable to Fig. 12a and b. The comparison between the X-Y system (Fig. 11a and b), and the X-U system (Fig.12a and b) highlights the spatial filtering characteristics of the ligand-receptor binding system, so modelled as a

Poisson-Binomial process. It indicates that the ligand-receptor binding system smoothens and modifies the gain of the molecular channel output Y. The ligand-receptor system also provides a more differentiated response at the receiver as can be observed in Fig. 12a and b, compared to Fig. 11a and b (for the diffusion-only channel).

In Fig. 13a and b, the bioequivalence measures for the input probability scenarios in Table II are presented. Let us take Liposome A as the reference system. It can be seen that Liposome A, B and C are equivalent, while Liposome D and E significantly deviate from the reference system, Liposome A. The filtering action of the ligand-receptor process can also be observed in the bioequivalence curve shown in Fig. 13b, where the system response in more smooth and at the same time accentuating the bioequivalence deviation of Liposome D and E from the reference system.

The discussions above are directly extendable to the results in Fig. 14-16, and Fig. 17-19 where higher channel degradation rates of k_d = 0.033 min^{-1} and k_d = 0.33 min^{-1}, respectively, are considered. These results consistently show that MI decreases with distance, and the filtering action of the ligand-receptor system is again reflected in the results. The use of MI as a bioequivalent measure is also decipherable from the results in Fig. 16 and19.

The implication of these observations is that in the design of a TDD system such as the one considered in this paper, the information-theoretic approach and associated metrics, such as the MI can offer unique insight for analysis. In the design aspect, MI metric suggests that the ligand-receptor design and operation can significantly influence the performance of a TDD system, and MC system in general. This could be achieve by varying the ligand-receptor association parameters such as the equilibrium constant, the residence time of ligand, and possibly the dimerization capability of the interactions.

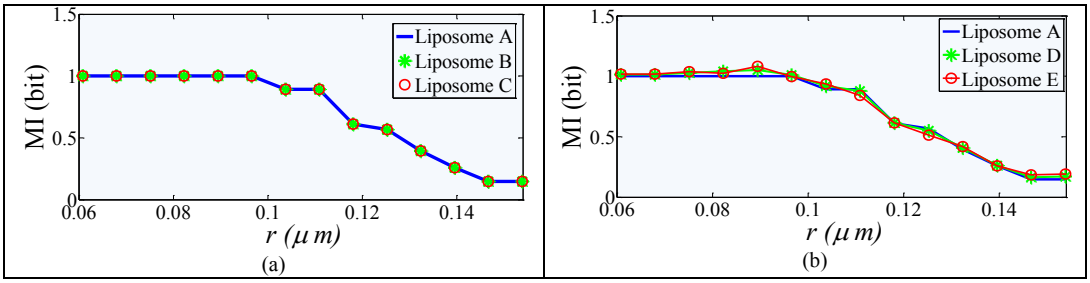

Fig. 11. MI as a function of distance r in the case where the effect of the nanocarrier error due to (a) false stimulation (Liposome A, B and C) and, (b) inadequate release (Liposome A, D and E) at k_d = 0.0033 min^{-1} is considered for X-Y system.

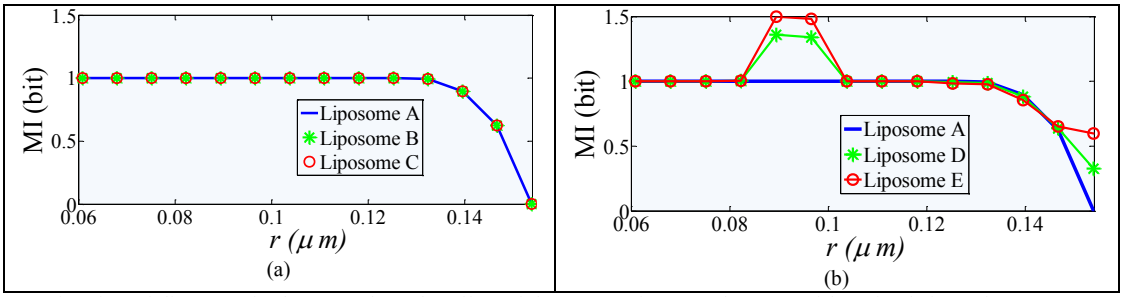

Fig. 12. MI as a function of distance r in the case where the effect of the nanocarrier error due to (a) false stimulation (Liposome A, B and C) and, (b) inadequate release (Liposome A, D and E) at k_d = 0.0033 min^{-1} is considered for X-U system.

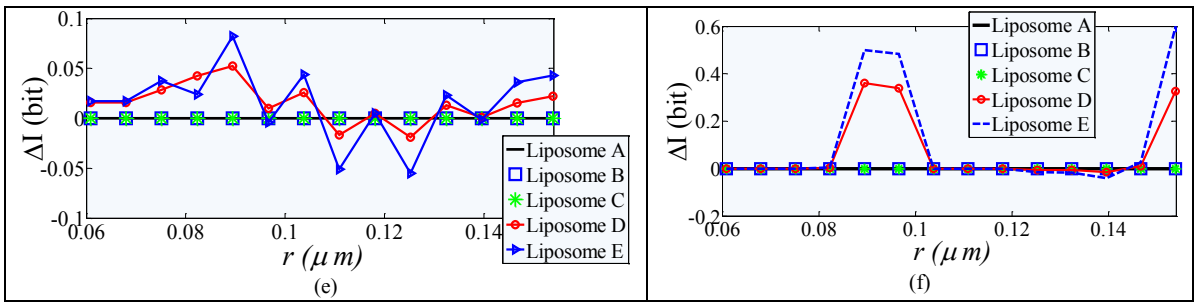

Fig. 13. Bioequivalence vs. distance for the input probability scenarios in Table II at k_d = 0.0033 min^{-1} for (a) diffusion-only channel (X-Y), and (b) diffusion-ligand-receptor channel (X-U).

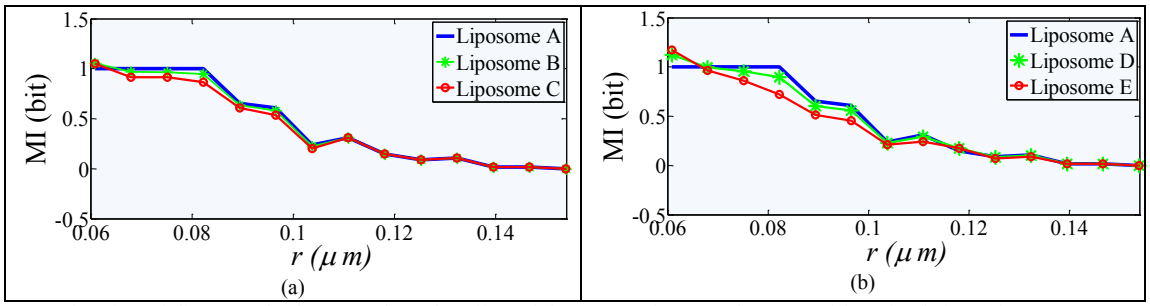

Fig. 14. MI as a function of distance r in the case where the effect of the nanocarrier error due to (a) false stimulation (Liposome A, B and C) and, (b) inadequate release (Liposome A, D and E) at $k_d = 0.033$ min^{-1} is considered for X-Y system.

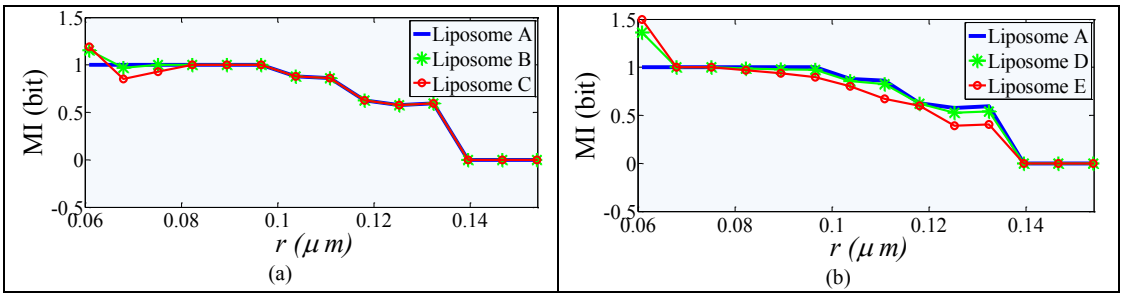

Fig. 15. MI as a function of distance r in the case where the effect of the nanocarrier error due to (a) false stimulation (Liposome A, B and C) and, (b) inadequate release (Liposome A, D and E) at $k_d = 0.033$ min^{-1} is considered for X-U system.

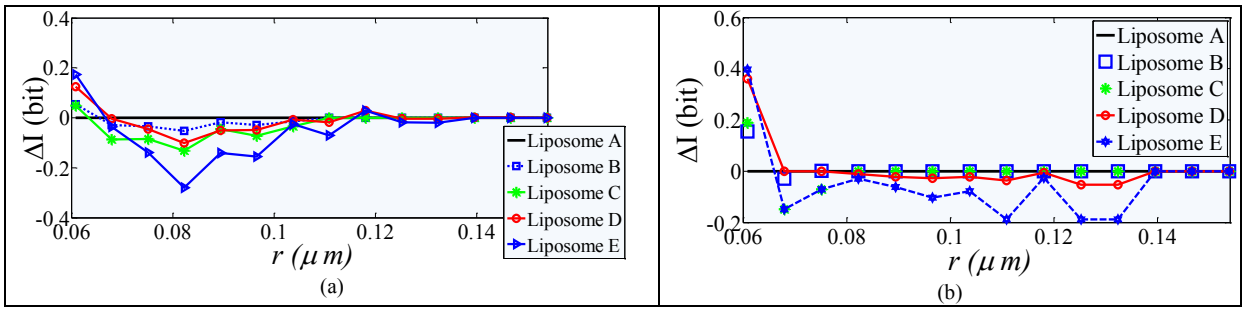

Fig. 16.Bioequivalence vs. distance for the input probability scenarios in Table II at $k_d = 0.033$ min^{-1} for (a) diffusion-only channel (X-Y), and (b) diffusion-ligand-receptor channel (X-U).

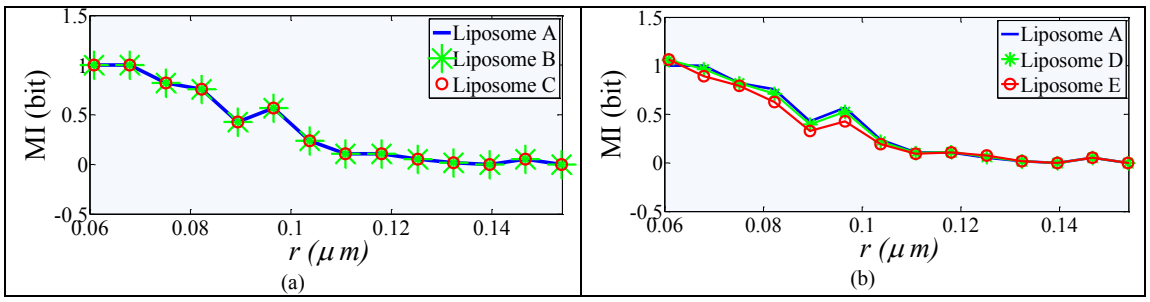

Fig. 17. MI as a function of distance r in the case where the effect of the nanocarrier error due to (a) false stimulation (Liposome A, B and C) and, (b) inadequate release (Liposome A, D and E) at $k_d = 0.33$ min^{-1} is considered for X-Y system.

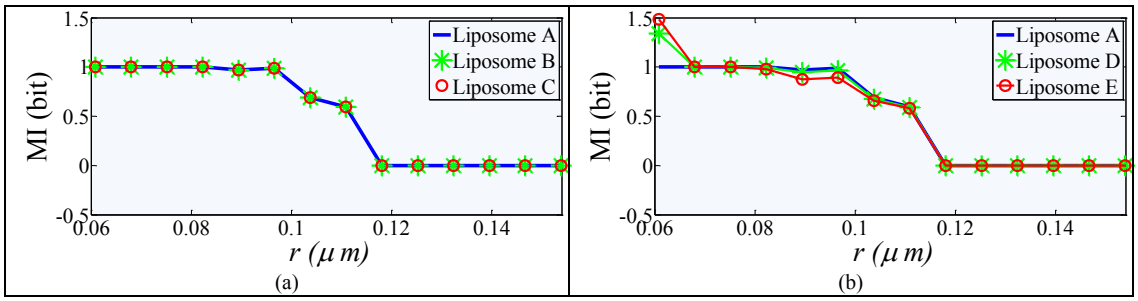

Fig. 18. MI as a function of distance r in the case where the effect of the nanocarrier error due to (a) false stimulation (Liposome A, B and C) and, (b) inadequate release (Liposome A, D and E) at $k_d = 0.33$ min^{-1} is considered for X-U system.

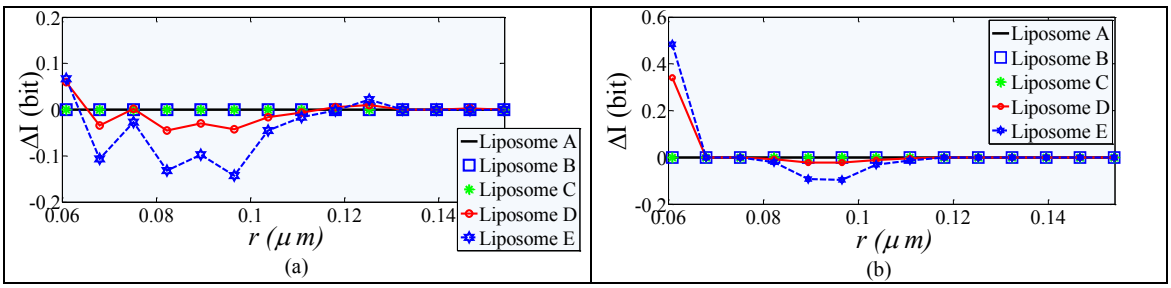

Fig. 19. Bioequivalence vs. distance for the input probability scenarios in Table II at $k_d = 0.33$ min^{-1} for (a) diffusion-only channel (X-Y), and (b) diffusion-ligand-receptor channel (X-U).

VIII. Conclusion

In this paper, we have presented an information-theoretic approach to the modeling and analysis of TDD. This approach takes the complexity, nonlinearity and multiscale characteristics of the TDD system into consideration in the model and analysis. Probability models for the molecular signal inputs, channels and outputs were presented. And the mutual information of the system was expressed. The mutual information measure is employed to derive an expression for the bioequivalence of the drug delivery modalities.

References

[1] J. Zhan, X. L. Ting, and J. Zhu, "The Research Progress of Targeted Drug Delivery Systems," in *IOP Conference Series: Materials Science and Engineering*, vol. 207, no.1, pp. 012017, 2017.

[2] M. Femminella, G. Reali, and A. V. Vasilakos, "A molecular communications model for drug delivery," *IEEE Trans NanoBiosci.,* vol. 14, pp. 935-945, 2015.

[3] Y. H. Bae and K. Park, "Targeted drug delivery to tumors: myths, reality and possibility," *J. Control Release,* vol. 153, no.3, pp. 198-205, 2011.

[4] U. Chude-Okonkwo, R. Malekian, and B. Maharaj, "Nanosystems and Devices for Advanced Targeted Nanomedical Applications," in *Advanced Targeted Nanomedicine*, ed: Springer, pp. 39-58, 2019.

[5] U. A. Chude-Okonkwo, R. Malekian, B. T. Maharaj, and A. V. Vasilakos, "Molecular Communication and Nanonetwork for Targeted Drug Delivery: A Survey," *IEEE Commun. Surveys & Tutorials,* vol. 19, no. 4, pp. 3046-3096, 2017.

[6] Y. Chahibi, M. Pierobon, S. O. Song, and I. F. Akyildiz, "A molecular communication system model for particulate drug delivery systems," *IEEE Trans.Biomed. Eng.,* vol. 60, no. 12, pp. 3468-3483, 2013.

[7] Y. Chahibi, I. F. Akyildiz, and S. O. Song, "Antibody-based molecular communication for targeted drug delivery systems," in *2014 36th Annual International Conference of the IEEE Engineering in Medicine and Biology Society*, pp. 5707-5710, 2014.

[8] U. A. Chude-Okonkwo, R. Malekian, and B. S. Maharaj, "Molecular communication model for targeted drug delivery in multiple disease sites with diversely expressed enzymes," *IEEE Trans.NanoBiosci.,* vol. 15, no. 3, pp. 230-245, 2016.

[9] T. Nakano, T. Suda, Y. Okaie, M. J. Moore, and A.V. Vasilakos, "Molecular communication among biological nanomachines: A layered architecture and research issues," *IEEE Trans. NanoBiosci,* vol. 13, no.3, pp. 169-197, 2014.

[10] T. Nakano, M. J. Moore, F. Wei, A.V. Vasilakos, J. Shuai, "Molecular communication and networking: Opportunities and challenges," *IEEE Trans. NanoBiosci.,* vol. 11, no. 2, pp. 135-148, 2012.

[11] P. A. Iglesias, "The use of rate distortion theory to evaluate biological signaling pathways," *IEEE Trans.Mol. Biol. Multi-Scale Commun.,* vol. 2, no. 1, pp. 31-39, 2016.

[12] A. Rhee, R. Cheong, and A. Levchenko, "The application of information theory to biochemical signaling systems," *Physical biology,* vol. 9, no. 4, pp. 31-39, 2012.

[13] C. Waltermann and E. Klipp, "Information theory based approaches to cellular signaling," *Biochimica et Biophysica Acta (BBA)-General Subjects,* vol. 1810, no. 10, pp. 924-932, 2011.

[14] B. W. Andrews and P. A. Iglesias, "An information-theoretic characterization of the optimal gradient sensing response of cells," *PLoS Computational Biology,* vol. 3, no. 8, pp. 1487-1497, 2007.

[15] N. M. Timme and C. Lapish, "A Tutorial for Information Theory in Neuroscience," *eNeuro,* vol. 5, no. 3, pp. 1-40, 2018.

[16] M. Pierobon and I. F. Akyildiz, "Capacity of a diffusion-based molecular communication system with channel memory and molecular noise," *IEEE Trans.Inform. Theo.,* vol. 59, no. 2, pp. 942-954, 2013.

[17] P. J. Thomas and A. W. Eckford, "Capacity of a simple intercellular signal transduction channel," *IEEE Tran. Inform. Theo.,* vol. 62, no. 12, pp. 7358-7382, 2016.

[18] D. B. Menendez, V. R. Senthivel, and M. Isalan, "Sender–receiver systems and applying information theory for quantitative synthetic biology," *Curr. opin. in Biotech.,* vol. 31, pp. 101-107, 2015.

[19] U. Chude-Okonkwo, R. Malekian, and B. Maharaj, "Understanding Delivery Routes and Operational Environments of Nanosystems," in *Advanced Targeted Nanomedicine*, ed: Springer, pp. 59-91, 2019.

[20] L. Felicetti, M. Femminella, G. Reali, T. Nakano, and A. V. Vasilakos, "TCP-like molecular communications," *IEEE J. Select Areas Commun.,* vol. 32, no. 12, pp. 2354-2367, 2014.

[21] V. Bhargava, "Forward error correction schemes for digital communications," *IEEE Commun. Mag.,* vol. 21, no. 1, pp. 11-19, 1983.

[22] M. S. Leeson and M. D. Higgins, "Forward error correction for molecular communications," *Nano Commun. Netw.,* vol. 3, no. 3, pp. 161-167, 2012.
[23] S. Qiu, T. Asyhari, and W. Guo, "Mobile molecular communications: Positional-distance codes," in *2016 IEEE 17th Intern. Worksh. Signal Proces. Adv. Wirel. Commun. (SPAWC)*, pp. 1-5, 2016.
[24] M. B. Dissanayake, Y. Deng, A. Nallanathan, E.M.N. Ekanayake, M. Elkashlan, "Reed solomon codes for molecular communication with a full absorption receiver," *IEEE Commun. Letters,* vol. 21, no. 6, pp. 1245-1248, 2017.
[25] T. Berger, "Living information theory," *IEEE Inform. Theo. Society Newsl.,* vol. 53, pp. 1-19, 2003.
[26] A. F. Molisch, *Wireless communications*: John Wiley & Sons, 2007.
[27] E. Grady, S. Böhm, K. McConalogue, A. Garland, J. Ansel, J. Olerud, and N. Bunnett, "Mechanisms attenuating cellular responses to neuropeptides: extracellular degradation of ligands and desensitization of receptors," *J Investi. Derm.Symp. Proc.*, vol. 2, no.1, pp. 69-75, 1997.
[28] S. Wilhelm, *et al.*, "Analysis of nanoparticle delivery to tumours," *Nature reviews materials,* vol. 1, no. 5, pp. 1-12, 2016.
[29] S. Panzeri, R. Senatore, M. A. Montemurro, and R. S. Petersen, "Correcting for the sampling bias problem in spike train information measures," *J. Neurophys.,* vol. 98, no.3, pp. 1064-1072, 2007.
[30] Y. Chahibi, M. Pierobon, and I. F. Akyildiz, "Pharmacokinetic modeling and biodistribution estimation through the molecular communication paradigm," *IEEE Trans. Biomed. Eng.,* vol. 62, no. 10, pp. 2410-2420, 2015.
[31] M. Eriksson, "Lattice-based simulations of microscopic reaction-diffusion models in a crowded environment," *Uppsala Universitet Conf. Proc.*, pp. 1-34, 2016.
[32] Z. Yin, Z. Wang, B. Liang, and L. Zhang, "Initial velocity effect on acceleration fall of a spherical particle through still fluid," *Mathematical Problems in Eng.,* vol. 2017, pp. 1-9, 2017.
[33] J. Zola, M. Aluru, A. Sarje, and S. Aluru, "Parallel information-theory-based construction of genome-wide gene regulatory networks," *IEEE Trans. Paral. Distrib. Sys.,* vol. 21, no. 12, pp. 1721-1733, 2010.
[34] S. C. Chow, "Bioavailability and bioequivalence in drug development," *Wiley Interdisc. Rev.: Computat. Stat.,* vol. 6, no. 4, pp. 304-312, 2014.
[35] W. Li, "Mutual information functions versus correlation functions," *J. Stat. Phys.,* vol. 60, no. 5-6 , pp. 823-837, 1990.
[36] S. A. Abraham, et. al., "The liposomal formulation of doxorubicin," in *Methods in enzym.*. vol. 391, ed: Elsevier, pp. 71-97, 2005.
[37] S. Ait-Oudhia, D. Mager, and R. Straubinger, "Application of pharmacokinetic and pharmacodynamic analysis to the development of liposomal formulations for oncology," *Pharmaceutics,* vol. 6, no. 1, pp. 137-174, 2014.
[38] S. Cascone, G. Lamberti, G. Titomanlio, and O. Piazza, "Pharmacokinetics of Remifentanil: a three-compartmental modeling approach," *Translational medicine@ UniSa,* vol. 7, pp. 18-22, 2013.
[39] C. Muratov, F. Posta, and S. Shvartsman, "Autocrine signal transmission with extracellular ligand degradation," *Physical biology,* vol. 6, no. 1, pp. 1-13, 2009.
[40] P. Bilalis, L.-A. Tziveleka, S. Varlas, and H. Iatrou, "pH-Sensitive nanogates based on poly (L-histidine) for controlled drug release from mesoporous silica nanoparticles," *Polymer Chemistry,* vol. 7, no. 7, pp. 1475-1485, 2016.
[41] R. A. Freitas Jr, "Nanomedicine FAQ," *Foresight Institute,* 1998.
[42] A. Bondi, "van der Waals volumes and radii," *The Journal of physical chemistry,* vol. 68, no. 3, pp. 441-451, 1964.